Journal of Inflammation Research

Dovepress
Taylor & Francis Group

Open Access Full Text Article

ORIGINAL RESEARCH

Distinct and Shared Molecular Mechanisms in Pediatric Antrochoanal Polyps and Chronic Rhinosinusitis with Nasal Polyps: A Proteomic and Metabolomic Integrative Analysis

Yong-Chao Chen, Xin Wang, Yan-Wen Pan, Yi-Shu Teng, Hong-Guang Pan

Department of Otorhinolaryngology, Shenzhen Children's Hospital, Shenzhen, Guangdong, People's Republic of China

Correspondence: Hong-Guang Pan, Department of Otorhinolaryngology, Shenzhen Children's Hospital, 7019 Yitian Road, Futian District, Shenzhen, Guangdong, 518038, People's Republic of China, Tel +86-18938691502, Email 1481717890@qq.com

Purpose: The underlying mechanisms of pediatric antrochoanal polyps (ACP)and chronic rhinosinusitis with nasal polyps (CRSwNP) remain largely unexplored. This study investigates their proteomic and metabolomic profiles to uncover unique and overlapping pathways, shedding light on their underlying causes.

Methods: Specimens were collected from six children with ACP, six with CRSwNP, and six with normal inferior turbinate mucosa (CK) at Shenzhen Children's Hospital. Protein profiles were analyzed using data-independent acquisition (DIA) mass spectrometry, while metabolite profiles were assessed via non-targeted metabolomics (UPLC-MS/MS). Differences in proteins and metabolites were identified through statistical selection and bioinformatics, followed by integrated pathway analysis to explore their roles in disease processes.

Results: Proteomic analysis identified 1000 differentially expressed proteins (DEPs) in ACP and 880 in CRSwNP compared to controls. Key DEPs in ACP included PEX1 and LYPD2, while CRSwNP included PEX1, CFAP52, SPAG6 and DHRS9. Metabolomic analysis identified 129 differential metabolites in ACP and 11 in CRSwNP, with 5-HTP showing opposite regulation between the two conditions. Pathway analysis pointed to oxidative stress and lipid metabolism disruptions in ACP, and immune and ciliary dysfunction in CRSwNP. Both conditions shared inflammation and extracellular matrix remodeling, but tryptophan metabolism diverged, with 5-HTP reduced in ACP and elevated in CRSwNP.

Conclusion: This study highlights oxidative stress and lipid dysregulation as hallmarks of pediatric ACP, distinct from ciliary and immune dysfunction in CRSwNP, with inflammation and matrix remodeling as common features. The opposing regulation of 5-HTP reflects differences in tryptophan metabolism. Key molecules like PEX1, LYPD2, CFAP52, and 5-HTP emerge as potential biomarkers, offering promise for improved diagnosis and targeted therapies in nasal polyp-related conditions, but the small sample size and exploratory design require validation in larger cohorts to ensure clinical applicability.

Keywords: maxillary sinus retro polyps, nasal polyps, proteomics, metabolomics, combined analysis, pediatrics

Introduction

Nasal polyps are benign polypoid lesions arising from the nasal or sinus mucosa, typically caused by chronic inflammation, tissue edema, or mucosal hyperplasia. Among these, antrochoanal polyps (ACP) and chronic rhinosinusitis with nasal polyps (CRSwNP) are the two major subtypes, each characterized by distinct pathological features and etiologies.[1,2] ACP, first described by Gustave Killian in 1906 and often referred to as Killian polyps, are solitary lesions predominantly originating from the maxillary sinus.[3] They extend through the natural or accessory ostium into the choana or nasopharynx, accounting for approximately 4–6% of all nasal polyps but are disproportionately represented in pediatric populations, constituting up to 33% of cases.[4] Clinically, ACPs present with unilateral nasal obstruction, postnasal drip, epistaxis, and snoring.[4,5] In contrast, CRSwNP, which originate bilaterally from the middle meatus, are

Received: 29 November 2024
Accepted: 22 March 2025
Published: 26 March 2025

characterized by bilateral nasal obstruction, anosmia, and a high prevalence of comorbidities such as allergic rhinitis, asthma, and aspirin-exacerbated respiratory disease (AERD).[6]

While clinical differences between ACP and CRSwNP are well-documented, their molecular distinctions remain elusive, particularly in children, where unique immune responses and developmental factors may shape disease mechanisms. Immunologically, ACP exhibits a type 1/3 inflammatory response, characterized by elevated IL-8 and interferon-γ (IFN-γ), driving a neutrophil-dominant inflammatory milieu.[7–9] In contrast, CRSwNP is hallmarked by a robust type 2 response, with increased levels of IL-4, IL-5, IL-13, and IgE, contributing to eosinophilic inflammation.[10,11] Both subtypes undergo tissue remodeling, partially mediated by the downregulation of tissue plasminogen activator (tPA), yet ACP exhibits a more pronounced suppression of tPA, suggesting a heightened propensity for fibrin deposition and edema compared to CRSwNP.[7,12] Additionally, distinct growth factor expression patterns further delineate these subtypes: ACP is associated with elevated levels of basic fibroblast growth factor (bFGF) and transforming growth factor-β (TGF-β) in the maxillary sinus mucosa,[13] potentially facilitating polyp formation, whereas CRSwNP pathology involves vascular endothelial growth factor (VEGF) and granulocyte-macrophage colony-stimulating factor (GM-CSF).[14] Despite these known differences, the precise molecular mechanisms differentiating ACP from CRSwNP remain poorly understood, particularly in pediatric populations.

Mass spectrometry-based proteomics and metabolomics offer powerful tools to address these gaps, enabling high-resolution mapping of proteins and metabolites to reveal disease-specific mechanisms.[15] In CRSwNP, proteomic studies have pinpointed biomarkers such as apolipoprotein E, periostin, and Mucin 5AC for diagnosis, and bone morphogenetic protein-2 as a prognostic marker for refractory cases.[15–19] Metabolomic analyses have identified maresins, linoleic acid, and specialized pro-resolving lipid mediators (SPM) as potential diagnostic or therapeutic targets, with oxidized glutathione (GSSG) linked to refractory CRSwNP prognosis.[15] Abnormal amino acid metabolism, mitochondrial dysfunction, and oxidative stress have also emerged as key features of CRSwNP pathogenesis.[17] However, a systematic, integrated proteomic and metabolomic analysis comparing ACP and CRSwNP—particularly in pediatric patients—remains lacking. Here, we apply proteomics and metabolomics to uncover distinct and shared molecular signatures of pediatric ACP and CRSwNP, aiming to bridge these research gaps. By identifying novel biomarkers and pathways, this study seeks to enhance disease classification and guide precision medicine. These insights could lead to improved diagnostic tools and targeted therapies, ultimately advancing clinical management of pediatric nasal polyps.

Methods

Patients and Tissue Samples

This study was approved by the Ethics Committee of Shenzhen Children's Hospital (No. 2023079) and conducted in accordance with the Declaration of Helsinki. Prior to enrollment, all participants or their legal guardians provided signed informed consent. Tissue samples were collected between January 2023 and December 2023 from three groups of pediatric patients aged 6–14 years. To ensure comparability and minimize potential confounding factors, the baseline characteristics of the ACP, CRSwNP, and CK groups were similar. (Table 1).

Inclusion criteria were as follows: (1) ACP group: Six patients diagnosed with antrochoanal polyps based on clinical presentation, nasal endoscopy, and imaging findings;[20] (2) CRSwNP group: Six patients diagnosed with bilateral chronic rhinosinusitis with nasal polyps, following the EPOS 2020 guidelines, with confirmation via endoscopic evaluation and CT imaging;[6] (3) Control (CK) group: Six samples of histologically normal inferior turbinate mucosa obtained

Table 1 Summary of Patient Characteristics

Characteristics	ACP	CRSwNP	CK	*P* value
Number of Patients	6	6	6	1.000
Gender (Male/Female)	3/3	3/3	3/3	1.000
Age (Mean ± SD)	9.67±1.97	9.83±2.32	9.67±1.97	0.987
Allergic rhinitis	1	3	1	0.330

Abbreviation: SD, standard deviation.

intraoperatively from the unaffected nasal cavities of ACP patients. Exclusion criteria included prior sinonasal surgery, systemic inflammatory or autoimmune diseases, or coexisting sinonasal conditions (eg, fungal sinusitis, malignancies). All specimens were obtained during functional endoscopic sinus surgery (FESS) under general anesthesia and stored at −80°C until analysis.

Non-Targeted Proteomics

Label-free data-independent acquisition (DIA) proteomics was conducted using high-resolution mass spectrometry to profile protein expression.[21] Proteins were extracted from tissue samples, digested with trypsin, and separated by liquid chromatography prior to analysis. Mass spectrometry was performed on a Q-Exactive HF-X system, with quality control ensured by running pooled samples every 10 runs to monitor instrument stability. Protein identification and quantification were executed using DIA-NN (v1.8)[22] with a false discovery rate (FDR) < 0.01. Data were normalized using median centering to account for systematic variation, and missing values were imputed using the k-nearest neighbors (k-NN) method. Principal component analysis (PCA) and partial least squares-discriminant analysis (PLS-DA) were applied to assess inter-group variability. Differentially expressed proteins (DEPs) were defined by a fold change (FC) > 1.5 or < 0.67 (1/1.5) and $p < 0.05$.

Non-Targeted Metabolomics

Untargeted metabolomics was performed using ultra-high-performance liquid chromatography-tandem mass spectrometry (UHPLC-MS/MS) in positive and negative ion modes.[23] Samples were processed with XCMS[23] for peak extraction, alignment, and integration, and metabolites were identified by matching spectra to the HMDB and KEGG databases. Quantification relied on extracted ion chromatogram (XIC) peak areas, with data normalized via total ion current (TIC) scaling in metaX[24] to adjust for batch effects. Quality control (QC) samples, prepared by pooling aliquots from all samples, were run every eight injections to assess reproducibility; features with coefficients of variation (CV) > 50% in QC samples were excluded. Missing values were handled by excluding features absent in >50% of samples per group. Differential metabolites were identified using Student's t-tests (FC > 1.5 or < 0.67, $p < 0.05$) and PLS-DA-derived Variable Importance in Projection (VIP) scores (> 1).

Combined Analysis

To integrate differential proteins and metabolites, pathway enrichment and network analyses were performed. Differentially expressed proteins and metabolites from ACP and CRSwNP groups were analyzed using Pathview[25] for KEGG pathway enrichment, identifying pathways jointly impacted across datasets and ranking them by statistical significance. Pathway diagrams were generated to visualize key metabolic and signaling processes.

For network analysis, the top 20 differentially expressed proteins and metabolites (ranked by p-value) were subjected to pairwise correlation analysis to identify potential co-regulatory interactions. Pearson correlation coefficients (≥0.6) were calculated, and networks were visualized using the igraph package in R.[26] Proteins and metabolites were represented as nodes, with node size proportional to eigenvector centrality, indicating their regulatory significance. Edges between nodes, representing correlations, were color-coded (blue for positive and red for negative correlations), with thickness indicating correlation strength.

Statistical Analysis

All statistical analyses were conducted using R software unless otherwise specified. Two-tailed t-tests or non-parametric equivalents were used for significance testing. PLS-DA was performed using the "mixOmics" package, and correlation network analyses were completed with the "igraph" package. Integrated pathway analysis and visualization were achieved with Pathview (https://pathview.uncc.edu/),[27] mapping differentially expressed proteins and metabolites onto KEGG pathways. The sample size (n=6 per group) reflects an exploratory study design, limiting statistical power and generalizability; future validation in larger cohorts is needed. All reported p-values are unadjusted unless specified, with FC > 1.5 selected to prioritize biologically meaningful changes despite the small sample size.

Results

Proteomics of ACP and CRSwNP

Label-free DIA proteomics of 18 tissue samples from ACP, CRSwNP, and CK groups identified 4908 unique proteins using DIA-NN (v1.8). PLS-DA analysis revealed distinct clustering among the three groups, indicating significant differences in proteomic profiles (Figure 1A).

Comparison of ACP and CK identified 1000 differentially expressed proteins (DEPs), including 512 upregulated and 488 downregulated proteins (Figure 1B). The top 10 DEPs (Table 2) included key proteins implicated in lipid metabolism, cellular signaling, and structural organization. Notably, PEX1 (Peroxisomal Biogenesis Factor 1), critical for lipid metabolism, was significantly downregulated, suggesting disrupted peroxisomal function. LYPD2 (Ly6/PLAUR Domain-Containing 2), highly upregulated, implicated epithelial remodeling and matrix regulation. HSD11B2 (Hydroxysteroid 11-Beta Dehydrogenase 2) and MYL4 (Myosin Light Chain 4), both downregulated, indicated disruptions in steroid metabolism and cytoskeletal organization.

In the CRSwNP group, 880 DEPs were identified compared to CK, with 532 upregulated and 346 downregulated proteins (Figure 1C). The top 10 DEPs (Table 3) shed light on pathways related to ciliary function, cytoskeletal integrity, and immune regulation. Among the top DEPs, PEX1 is a crucial component in peroxisome assembly, playing a pivotal role in lipid metabolism and the regulation of reactive oxygen species (ROS). Its downregulation suggests impaired peroxisomal function, which may exacerbate oxidative stress and contribute to the chronic inflammatory environment seen in CRSwNP. CFAP52 (Cilia and Flagella Associated Protein 52) and SPAG6 (Sperm Associated Antigen 6) were highly upregulated, emphasizing the role of ciliary dysfunction and cytoskeletal stability. LYPD2, shared with ACP, highlighted common epithelial remodeling mechanisms, while DHRS9 (Dehydrogenase/Reductase 9) suggested involvement in metabolic and inflammatory pathways.

Venn diagram analysis (Figure 1D) identified 594 shared proteins between ACP and CRSwNP, suggesting overlapping pathways, particularly in extracellular matrix remodeling and inflammation. Heatmap analysis (Figure 1E) further confirmed condition-specific clustering and unique proteomic signatures. Notably, PEX1 and CFAP52 exemplified disruptions unique to ACP and CRSwNP, respectively. These findings reveal shared and distinct molecular mechanisms in ACP and CRSwNP.

Metabolomic of ACP and CRSwNP

Non-targeted metabolomics analysis using LC-MS/MS identified 21,327 compounds across ACP, CRSwNP, and CK tissue samples. Partial Least Squares Discriminant Analysis (PLS-DA) revealed distinct clustering patterns, indicating significant metabolic differences among the three groups (Figure 2A).

Based on significance criteria of FC > 1.5 or FC < 1/1.5, in conjunction with VIP > 1 and $p < 0.05$, we identified 129 differentially expressed metabolites between the ACP and CK groups, with 102 metabolites upregulated and 27 downregulated (Figure 2B); detailed information on the top 10 metabolites can be found in Table 4. Key DEMs included DL-2-Fluorophenylglycine, suggesting its role in amino acid metabolism and inflammatory responses, and Tetrahydrothiophene sulfoxide, reflecting altered sulfur metabolism and oxidative stress regulation.

For CRSwNP, 11 DEMs were identified compared to CK, with 10 upregulated and 1 downregulated (Figure 2C). Notable DEMs (Table 5) included myo-Inositol, associated with epithelial remodeling and osmotic regulation, and tyrosine, suggesting disruptions in immune modulation and protein metabolism.

Venn diagram analysis (Figure 2D) identified four metabolites shared between ACP and CRSwNP: Quinaldic acid, 5-Hydroxy-L-tryptophan (5-HTP), Vasicinone, and Spermine. These metabolites represent overlapping pathways potentially linked to inflammation and cellular repair. Notably, 5-HTP was oppositely regulated, being downregulated in ACP and upregulated in CRSwNP, reflecting distinct serotonergic activities in the two conditions. Heatmap analysis (Figure 2E) confirmed the separation among the ACP, CRSwNP, and CK groups, as well as extensive co-regulation of metabolites within each condition, consistent with the PLS-DA findings.

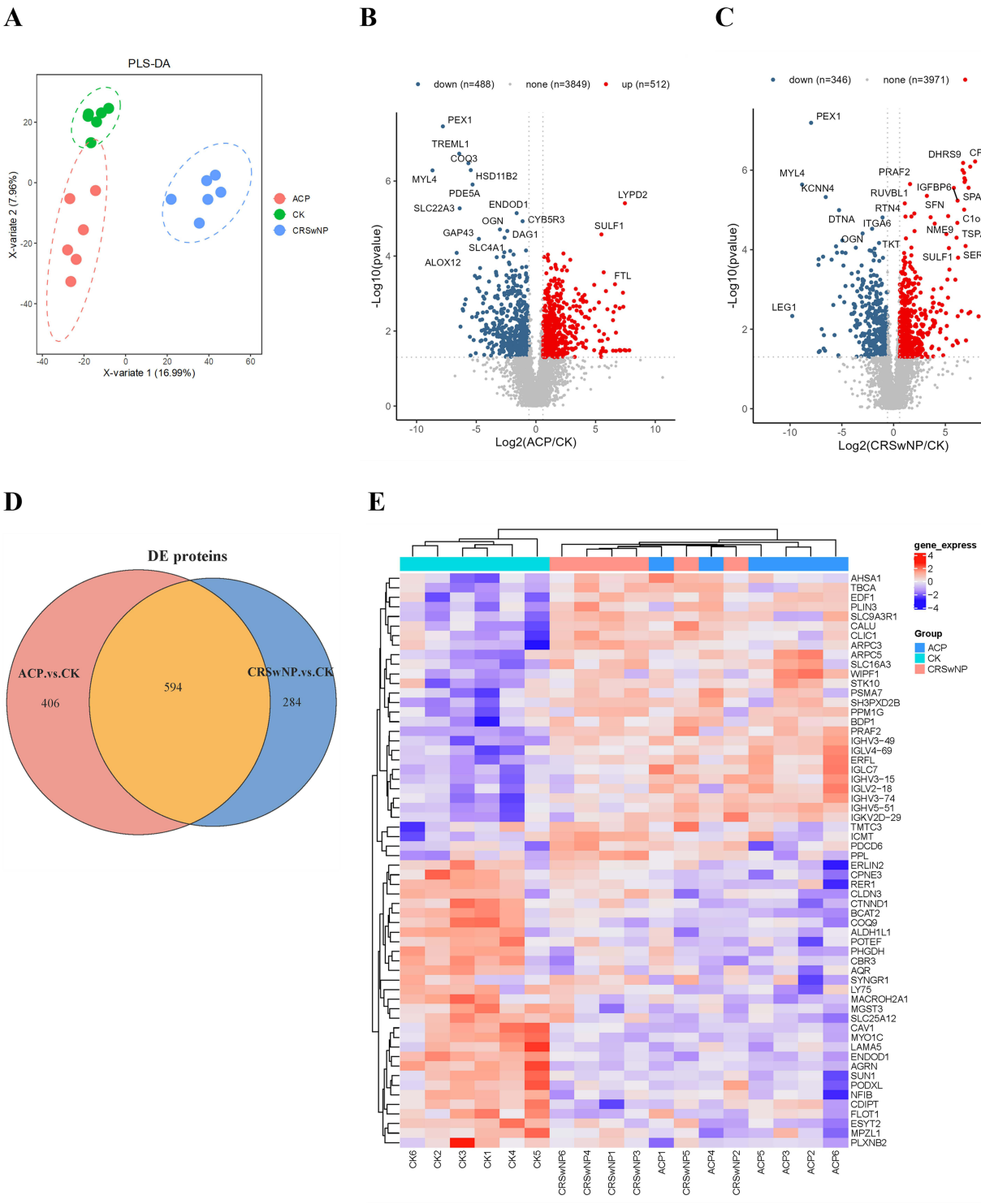

Figure 1 Differential analysis in protein expression levels between ACP or CRSwNP and CK. (**A**) PLS-DA of proteomic data in ACP, CRSwNP and CK. (**B**) Volcano plot of ACP vs CK proteins. (**C**) Volcano plot of CRSwNP vs CK proteins. (**D**) Venn diagram summarising the differential and overlapping proteins. (**E**) Multigroup heatmap with dendrogram of DE protein levels incorporating ACP, CRSwNP and CK.

https://doi.org/10.2147/JIR.S507475

Table 2 Top 10 DE Proteins in ACP vs CK

Protein	Log2 FC	FC	*P* value
PEX1	−7.7982	0.004493	3.48×10^{-8}
TREML1	−6.42704	0.011622	1.86×10^{-7}
COQ3	−5.6555	0.019839	3.35×10^{-7}
HSD11B2	−5.45869	0.022739	5.11×10^{-7}
MYL4	−8.66729	0.00246	5.20×10^{-7}
PDE5A	−5.3103	0.025202	1.24×10^{-7}
LYPD2	7.457825	175.8041	3.91×10^{-6}
SLC22A3	−6.38939	0.011929	5.34×10^{-6}
ENDOD1	−1.6143	0.326624	7.18×10^{-6}
CYB5R3	−1.11643	0.461234	1.18×10^{-5}

Abbreviations: FC, fold change; DE, differentially expressed.

Table 3 Top 10 DE Proteins in CRSwNP vs CK

Protein	Log2 FC	FC	*P* value
PEX1	−7.971	0.003986	6.44×10^{-8}
CFAP52	7.876031	234.9208	6.04×10^{-7}
DHRS9	6.717855	105.2631	6.58×10^{-7}
LYPD2	7.400836	168.9949	8.17×10^{-7}
ROPN1L	6.657035	100.9177	9.97×10^{-7}
CAPSL	6.802022	111.5868	1.16×10^{-6}
SPAG6	6.843742	114.8607	1.59×10^{-6}
EFHC2	6.917381	120.8757	1.78×10^{-6}
FZD2	6.856313	115.866	1.98×10^{-6}
PRAF2	1.58976	3.009992	2.23×10^{-6}

Abbreviations: FC, fold change; DE, differentially expressed.

Pathway Analyses

An integrated proteomic and metabolomic analysis based on KEGG pathway annotation revealed significant metabolic reprogramming in ACP and CRSwNP compared to normal controls (Figure 3). This analysis identified both shared and distinct pathways, highlighting key differences in the metabolic landscapes of these conditions.

In ACP, 34 pathways were enriched with differential proteins and metabolites (Figure 3A), including tryptophan metabolism, beta-alanine metabolism, valine, leucine, and isoleucine degradation, fatty acid degradation, and lysine degradation. These pathways reflect extensive alterations in amino acid, lipid, and energy metabolism, underscoring the metabolic shifts associated with inflammation and structural remodeling in ACP tissues. In CRSwNP, 37 enriched pathways were identified (Figure 3B), with notable involvement in protein digestion and absorption, serotonergic synapse, purine metabolism, tryptophan metabolism, and beta-alanine metabolism. These pathways highlight disruptions in protein turnover, nucleotide synthesis.

Tryptophan metabolism emerged as a shared but distinctly regulated pathway between ACP and CRSwNP (Figures 3C and D). While associated proteins showed consistent regulation, significant differences were observed in metabolite profiles. Notably, 5-HTP, a serotonin precursor, was markedly upregulated in CRSwNP, reflecting enhanced serotonin production and its role in driving inflammation and tissue remodeling. Conversely, 5-HTP was downregulated in ACP, suggesting a metabolic shift favoring the kynurenine pathway, known for its association with oxidative stress and immune modulation.

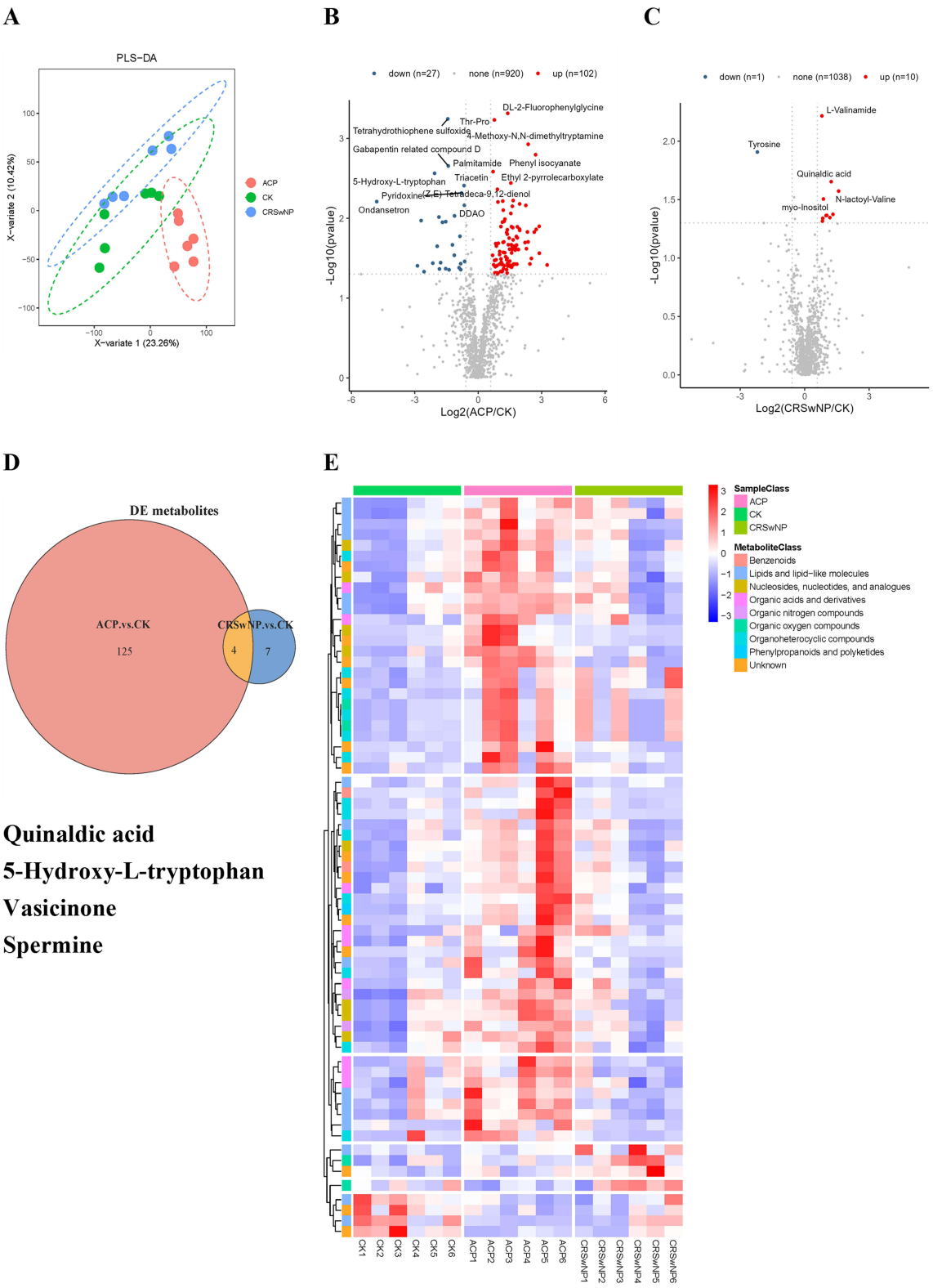

Figure 2 Differential analysis in metabolite abundance levels between ACP or CRSwNP and CK. (**A**) PLS-DA of metabolomic data in ACP, CRSwNP and CK. (**B**) Volcano plot of ACP vs CK metabolites. (**C**) Volcano plot of CRSwNP vs CK metabolites. (**D**) Venn diagram summarising the differential and overlapping metabolites. (**E**) Multigroup heatmap with dendrogram of DE metabolite levels incorporating ACP, CRSwNP and CK.

https://doi.org/10.2147/JIR.S507475

Table 4 Top 10 DE Metabolites in ACP vs CK

Metabolite	Log2 FC	FC	*P* value
DL-2-Fluorophenylglycine	1.396096	2.631885	4.85×10^{-4}
Tetrahydrothiophene sulfoxide	−1.43779	0.369131	5.70×10^{-4}
Thr-Pro	0.764049	1.698251	5.86×10^{-4}
4-Methoxy-N, N-dimethyltryptamine	2.362669	5.143209	1.18×10^{-3}
Phenyl isocyanate	2.712717	6.555552	1.60×10^{-3}
Gabapentin related compound D	−1.41529	0.374935	2.21×10^{-3}
Palmitamide	0.701587	1.626293	2.61×10^{-3}
5-Hydroxy-L-tryptophan	−2.06527	0.238941	2.73×10^{-3}
Ethyl 2-pyrrolecarboxylate	1.54271	2.913412	3.61×10^{-3}
Triacetin	−0.66899	0.628945	3.90×10^{-3}

Abbreviations: FC, fold change; DE, differentially expressed.

Table 5 11 DE Metabolites in CRSwNP vs CK

Metabolite	Log2 FC	FC	P value
L-Valinamide	0.801808	1.743284	6.08×10^{-3}
Tyrosine	−2.20166	0.217387	1.24×10^{-2}
Quinaldic acid	1.23439	2.352818	2.22×10^{-2}
N-lactoyl-Valine	1.579826	2.989337	2.67×10^{-2}
myo-Inositol	0.871417	1.829459	3.12×10^{-2}
1-O-Hexadecyl-2-O-(4Z,7Z,10Z,13Z,16Z,19Z-docosahexaenoyl)-sn-glyceryl-3-phosphorylcholine	1.317077	2.491607	4.22×10^{-2}
5-Hydroxy-L-tryptophan	1.028836	2.040377	4.31×10^{-2}
Vasicinone	0.994704	1.992672	4.33×10^{-2}
Cholesterol	1.172218	2.253579	4.51×10^{-2}
Spermine	0.840431	1.790585	4.57×10^{-2}
Stearamide	1.772768	0.826004	4.83×10^{-2}

Abbreviations: FC, fold change; DE, differentially expressed.

Network Analyses

To uncover integrated relationships between differential proteins and metabolites, we performed pairwise correlation network analysis using the top 20 DE proteins and metabolites, selected based on the lowest p-values. This analysis aimed to reveal key co-regulatory interactions in ACP and CRSwNP (Figure 4A and B). In the ACP network (Figure 4A), significant negative correlations were observed between lipid metabolism proteins (PEX1, HSD11B2) and metabolites like DL-2-Fluorophenylglycine and Thr-Pro, suggesting disruptions in oxidative stress regulation. LYPD2 exhibited strong positive correlations with Phenyl isocyanate and Palmitamide, highlighting its role in epithelial remodeling. The CRSwNP network (Figure 4B) revealed strong positive correlations between CFAP52 and lipid-associated metabolites (Cholesterol, myo-Inositol), indicating enhanced lipid signaling and epithelial function. The positive association of SPAG6 with 5-Hydroxy-L-tryptophan suggests its involvement in serotonin metabolism and ciliary dysfunction, key features of CRSwNP. These networks provide novel evidence of integrated molecular drivers, though validation in larger cohorts is essential to confirm their clinical utility as biomarkers.

Discussion

This study provides the first comprehensive integration of proteomic and metabolomic data to elucidate molecular differences between ACP and CRSwNP in pediatric patients. Distinct proteomic and metabolomic profiles were identified, revealing both unique and shared mechanisms underlying these conditions.

Our findings highlight substantial differences in protein and metabolite profiles between ACP and CRSwNP, underscoring the unique pathological features of these conditions. ACP, traditionally considered a benign lesion originating

A

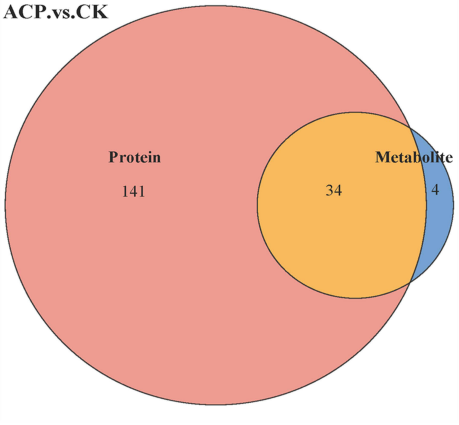

Top 5 significant pathways :

Tryptophan metabolism

beta-Alanine metabolism

Valine, leucine and isoleucine degradation

Fatty acid degradation

Lysine degradation

B

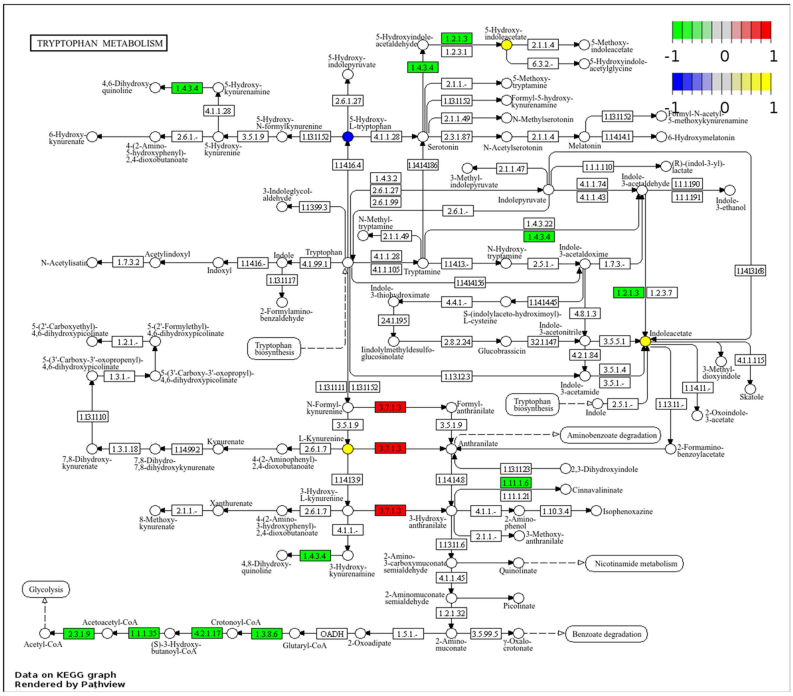

C

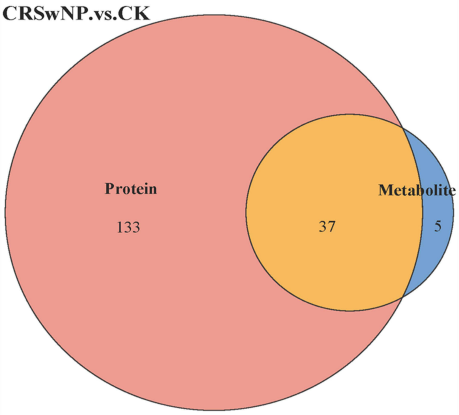

Top 5 significant pathways :

Protein digestion and absorption

Serotonergic synapse

Purine metabolism

Tryptophan metabolism

beta-Alanine metabolism

D

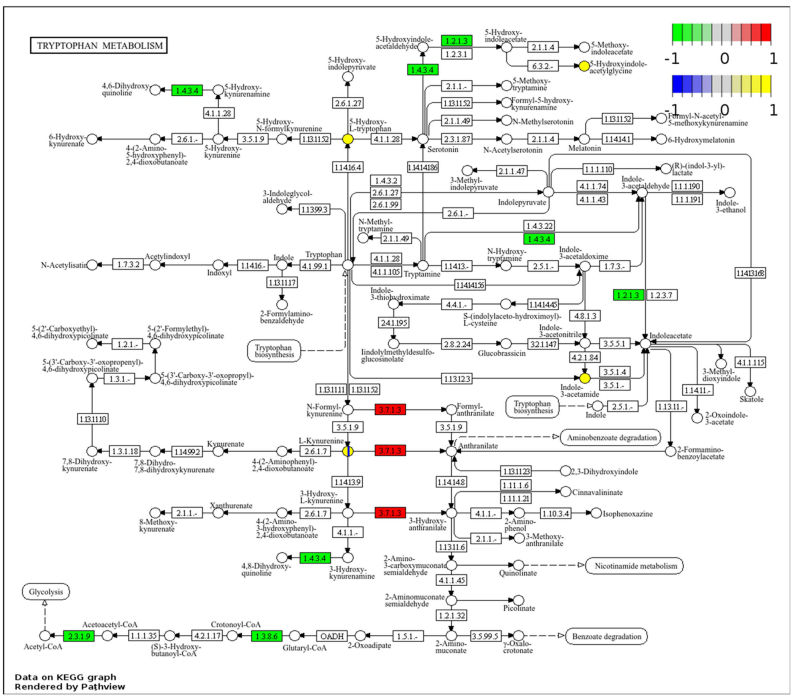

Figure 3 Pathways analysis. (**A**) Venn diagrams illustrating the number of metabolite and protein pathways significantly changed in ACP vs CK, followed by list of top 5 significant pathways in ACP vs CK that were regulated at both the protein and metabolite level. (**B**) Venn diagrams illustrating the number of metabolite and protein pathways significantly changed in CRSwNP vs CK, followed by list of top 5 significant pathways in CRSwNP vs CK that were regulated at both the protein and metabolite level. (**C**) Illustrative example of protein and metabolite changes in tryptophan metabolism in ACP vs CK. (**D**) Illustrative example of protein and metabolite changes in tryptophan metabolism in CRSwNP vs CK.

https://doi.org/10.2147/JIR.S507475

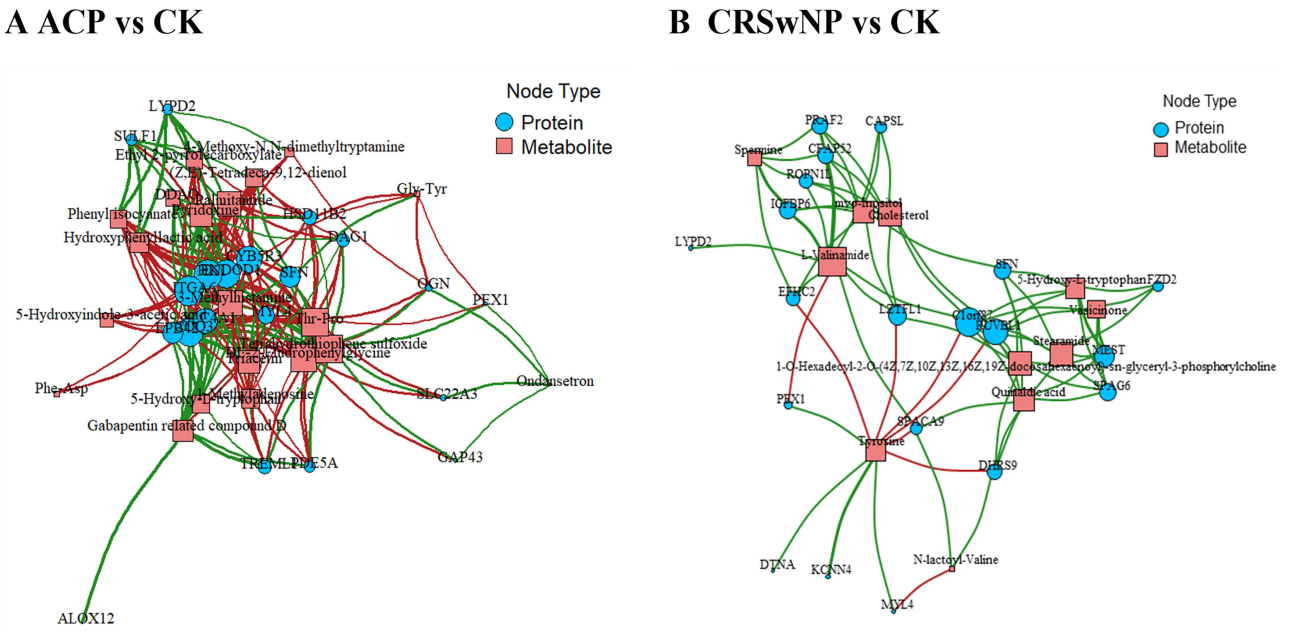

Figure 4 Network analysis. (**A**) Network analyses illustrating functional protein (circles) and metabolite (squares) nodes in ACP vs CK. (**B**) Network analyses illustrating functional protein (circles) and metabolite (squares) nodes in CRSwNP vs CK.

from the maxillary sinus, exhibited marked disruptions in lipid metabolism, as evidenced by the significant downregulation of PEX1 and HSD11B2. These proteins are critical for peroxisomal function and steroid metabolism, respectively, suggesting impaired lipid processing and oxidative stress regulation in ACP tissues. The downregulation of PEX1 is particularly noteworthy, as it may contribute to the accumulation of ROS, exacerbating local oxidative damage and promoting epithelial remodeling.[28] This aligns with the upregulation of LYPD2, which was strongly correlated with metabolites involved in structural reorganization, such as phenyl isocyanate and palmitamide. Together, these observations suggest that epithelial remodeling and oxidative stress are central to ACP pathophysiology, potentially driven by impaired peroxisomal and steroid metabolism. These findings align with previous studies suggesting epithelial remodeling and oxidative stress as key features in nasal polyps.[8,29,30] However, the exact role of oxidative stress in ACP remains debated. However, conflicting evidence exists; Yuce Islamoglu et al found no significant differences in oxidative stress markers (eg, thiols, ischemic modified albumin) between ACP patients and controls,[31] suggesting oxidative stress may be context-specific rather than a primary driver. Our data, enriched by pediatric specificity, offer novel insights into these mechanisms.

In contrast, the proteomic and metabolomic landscape of CRSwNP was characterized by peroxisomal dysfunction, ciliary abnormalities, and immune dysregulation. PEX1, a protein critical for peroxisomal biogenesis, was significantly downregulated in CRSwNP, consistent with previous bioinformatics studies identifying peroxisomal dysfunction as a hallmark of the disease.[32] Peroxisomes are essential for lipid metabolism and reactive oxygen species (ROS) regulation, and the loss of PEX1 likely exacerbates oxidative stress, disrupting lipid homeostasis and compromising epithelial function. This peroxisomal impairment may further amplify inflammation, as ROS imbalances activate immune signaling pathways that perpetuate tissue damage and inflammatory responses. Intriguingly, PEX6, another key peroxisomal protein, was identified as a hub gene in CRSwNP, highlighting the extensive impact of peroxisomal dysregulation on disease pathophysiology.[32] Additionally, upregulated proteins such as CFAP52 and SPAG6 indicated significant alterations in ciliary architecture and function, which align with the clinical manifestations of CRSwNP, including severe nasal obstruction and impaired mucociliary clearance. These findings corroborate recent studies linking cilia loss and reduced motility to key pathological processes in CRSwNP.[33] Our metabolomic analysis further identified a substantial increase in myo-inositol and cholesterol levels, metabolites intimately tied to lipid signaling and membrane homeostasis. The elevated levels of these metabolites, alongside the upregulation of ciliary-associated proteins, suggest an adaptive

metabolic response aimed at maintaining epithelial barrier integrity amidst persistent inflammation. Additionally, the involvement of DHRS9, a pivotal enzyme in retinoid metabolism, underscores the interplay between immune modulation and epithelial barrier repair mechanisms in CRSwNP. Given the role of retinoid signaling in epithelial differentiation and immune homeostasis, the altered expression of DHRS9 may reflect an attempt to restore epithelial functionality, thereby counterbalancing the chronic inflammatory milieu. The observed dysregulation of cytokines like IL-17A and IL-22, which activate pathways such as Hippo-YAP, further corroborates the notion of disrupted epithelial repair processes, contributing to the pathogenesis of CRSwNP.[34]

Despite their distinct molecular signatures, ACP and CRSwNP share several overlapping pathways, particularly those involved in extracellular matrix remodeling and inflammation. The shared upregulation of LYPD2 across both conditions underscores a common mechanism of epithelial adaptation in response to chronic inflammatory stimuli. This protein, known for its role in cell surface signaling and matrix interactions, likely contributes to the structural changes observed in the nasal mucosa of both ACP and CRSwNP patients.

The identification of commonly regulated metabolites, including quinaldic acid, vasicinone, and spermine, highlights shared metabolic adaptations that facilitate cellular repair and inflammatory resolution. These metabolites are known for their roles in modulating oxidative stress and inflammatory signaling, suggesting that both ACP and CRSwNP engage similar compensatory mechanisms to counteract the chronic inflammatory milieu. However, our data also revealed divergent regulation of 5-HTP, a precursor of serotonin. In CRSwNP, 5-HTP was significantly upregulated, suggesting enhanced serotonin production, which may drive inflammation and contribute to tissue remodeling via serotonergic signaling pathways. Conversely, the downregulation of 5-HTP in ACP points to a metabolic shift favoring the kynurenine pathway, potentially as an adaptive response to mitigate oxidative stress through increased production of NAD+ precursors.

The molecular differences between ACP and CRSwNP may stem from their distinct anatomical origins and immune profiles. ACP originates in the maxillary sinus and demonstrates a solitary presentation, whereas CRSwNP involves bilateral middle meatus inflammation with systemic Th2-skewed immune responses. Lymphatic obstruction, as hypothesized by Mostafa, may further drive the T1-dominant inflammation and structural remodeling observed in ACP.[8,35] Additionally, pediatric immune system immaturity may influence the distinct inflammatory patterns observed in ACP,[8,36] enhancing the study's relevance to age-specific disease mechanisms. The identification of potential biomarkers (eg, PEX1, LYPD2, CFAP52, 5-HTP) offers significant clinical implications, such as differentiating ACP from CRSwNP for diagnosis or targeting oxidative stress and ciliary function for therapy. However, practical translation remains preliminary; for instance, PEX1 could guide antioxidant therapies, while CFAP52 might inform ciliary-targeted interventions, but these require functional validation.

This study has several limitations. The small sample size restricts generalizability, and the absence of an independent validation cohort reduces the robustness of the findings. Additionally, mass spectrometry approaches may miss low-abundance proteins and metabolites, necessitating advanced analytical techniques and larger cohorts for validation. Future research should focus on validating potential biomarkers such as PEX1, 5-HTP, LYPD2 and CFAP52 using larger, independent cohorts and functional assays. Multi-omics approaches integrating transcriptomics, microbiome analysis, and environmental factors could provide a more comprehensive understanding of ACP and CRSwNP pathogenesis. Further investigation into the role of oxidative stress, particularly in relation to inflammatory pathways, will also be essential.

Conclusions

This study uncovers distinct and shared molecular mechanisms in pediatric ACP and CRSwNP via proteomic and metabolomic analyses. ACP features oxidative stress and lipid metabolism deficits, while CRSwNP shows ciliary dysfunction and immune dysregulation. Shared pathways include inflammation and matrix remodeling, with divergent tryptophan metabolism (5-HTP downregulated in ACP, upregulated in CRSwNP). Potential biomarkers (PEX1, LYPD2, CFAP52, 5-HTP) offer promise for precision diagnosis and treatment, but the small sample size and exploratory design require validation in larger cohorts to ensure clinical applicability.

Data Sharing Statement

The datasets used and/or analyzed during the current study are available from the corresponding author on reasonable request.

Ethics Approval and Consent to Participate

This study was approved by the Ethics Committee of Shenzhen Children's Hospital (No. 2023079) and complied with the Declaration of Helsinki. Informed consent was obtained from all study participants or their legal guardians prior to study commencement.

Acknowledgments

The authors are extremely grateful for the enthusiasm and time provided by the parents and participants in this study.

Author Contributions

All authors made a significant contribution to the work reported, whether that is in the conception, study design, execution, acquisition of data, analysis and interpretation, or in all these areas; took part in drafting, revising or critically reviewing the article; gave final approval of the version to be published; have agreed on the journal to which the article has been submitted; and agree to be accountable for all aspects of the work.

Funding

This work was supported by Shenzhen Municipal Science and Technology Innovation Committee (no. JCYJ 202308073000474) and Guangdong High-level Hospital Construction Fund Clinical Research Project of Shenzhen Children's Hospital (no. LCYJ2022063).

Disclosure

All authors declare that they have no conflicts of interest in this work.

References

1. Honkanen T, Luukkainen A, Lehtonen M, et al. Indoleamine 2,3-dioxygenase expression is associated with chronic rhinosinusitis with nasal polyps and antrochoanal polyps. *Rhinology*. 2011;49(3):356–363. doi:10.4193/Rhino10.191
2. Luukkainen A, Seppälä M, Renkonen J, et al. Low lymphatic vessel density associates with chronic rhinosinusitis with nasal polyps. *Rhinology*. 2017;55(2):181–191. doi:10.4193/Rhin16.007
3. Maldonado M, Martínez A, Alobid I, Mullol J. The antrochoanal polyp. *Rhinology*. 2004;42(4):178–182.
4. Frosini P, Picarella G, De Campora E. Antrochoanal polyp: analysis of 200 cases. *Acta Otorhinolaryngologica Italica*. 2009;29(1):21–26.
5. Veerappan I, Ramar R, Navaneethan N, Dharmapuri Yaadhavakrishnan RP. Antrochoanal polyp presenting as obstructive sleep apnea. *Indian J Pediatr*. 2013;80(11):959–961. doi:10.1007/s12098-012-0876-8
6. Fokkens WJ, Lund VJ, Hopkins C, et al. European position paper on rhinosinusitis and nasal polyps 2020. *Rhinology*. 2020;58(1):1–464. doi:10.4193/Rhin20.401
7. Chen CL, Wang YT, Yao Y, et al. Inflammatory endotypes and tissue remodeling features in antrochoanal polyps. *Allergy Asthma Immunol Res*. 2021;13(6):863–881. doi:10.4168/aair.2021.13.6.863
8. Garaycochea O, Van Strahlen CR, Alobid I, Mullol J. Pheno-endotyping antrochoanal nasal polyposis. *Curr Allergy Asthma Reports*. 2023;23(3):165–180. doi:10.1007/s11882-023-01066-1
9. Zheng H, Tang L, Song B, et al. Inflammatory patterns of antrochoanal polyps in the pediatric age group. *Allergy Asthma Clin Immunol*. 2019;15(1):39. doi:10.1186/s13223-019-0352-3
10. Striz I, Golebski K, Strizova Z, et al. New insights into the pathophysiology and therapeutic targets of asthma and comorbid chronic rhinosinusitis with or without nasal polyposis. *Clin Sci*. 2023;137(9):727–753. doi:10.1042/CS20190281
11. Shah SA, Kobayashi M. Pathogenesis of chronic rhinosinusitis with nasal polyp and a prominent T2 endotype. *Heliyon*. 2023;9:e19249.
12. Hulse KE, Stevens WW, Tan BK, Schleimer RP. Pathogenesis of nasal polyposis. *Clin Experim Allergy*. 2015;45(2):328–346. doi:10.1111/cea.12472
13. Mahfouz ME, Elsheikh MN, Ghoname NF. Molecular profile of the antrochoanal polyp: up-regulation of basic fibroblast growth factor and transforming growth factor beta in maxillary sinus mucosa. *Am J Rhinol*. 2006;20(4):466–470. doi:10.2500/ajr.2006.20.2894
14. Divekar RD, Samant S, Rank MA, et al. Immunological profiling in chronic rhinosinusitis with nasal polyps reveals distinct VEGF and GM - CSF signatures during symptomatic exacerbations. *Clin Experim Allergy*. 2015;45(4):767–778. doi:10.1111/cea.12463
15. Guo S, Tian M, Fan Y, Zhang X. Recent advances in mass spectrometry-based proteomics and metabolomics in chronic rhinosinusitis with nasal polyps. *Front Immunol*. 2023;14:1267194. doi:10.3389/fimmu.2023.1267194

16. Xie S, Zhang H, Liu Y, et al. The role of serum metabolomics in distinguishing chronic rhinosinusitis with nasal polyp phenotypes. *Front Mol Biosci*. 2020;7:593976. doi:10.3389/fmolb.2020.593976
17. Yang Y, Guo J, Yao Y, et al. Proteomics and metabolomics analysis of nasal lavage fluid in chronic rhinosinusitis with nasal polyps. *Int Forum Allergy Rhinol*. 2023;13:1966–1970.
18. Workman AD, Kohanski MA, Cohen NA. Biomarkers in chronic rhinosinusitis with nasal polyps. *Immunol Allergy Clin North America*. 2018;38 (4):679–692. doi:10.1016/j.iac.2018.06.006
19. Kim JY, Lim S, Lim HS, et al. Bone morphogenetic protein-2 as a novel biomarker for refractory chronic rhinosinusitis with nasal polyps. *J Allergy Clin Immunol*. 2021;148(2):461–472.e413. doi:10.1016/j.jaci.2021.02.027
20. Yaman H, Yilmaz S, Karali E, Guclu E, Ozturk O. Evaluation and management of antrochoanal polyps. *Clin Experim Otorhinolaryngol*. 2010;3 (2):110–114. doi:10.3342/ceo.2010.3.2.110
21. Bruderer R, Bernhardt OM, Gandhi T, et al. Extending the limits of quantitative proteome profiling with data-independent acquisition and application to Acetaminophen-treated three-dimensional liver microtissues. *mol Cellular Proteomics*. 2015;14:1400–1410.
22. Demichev V, Messner CB, Vernardis SI, Lilley KS, Ralser M. DIA-NN: neural networks and interference correction enable deep proteome coverage in high throughput. *Nat Methods*. 2020;17(1):41–44. doi:10.1038/s41592-019-0638-x
23. Want EJ, Masson P, Michopoulos F, et al. Global metabolic profiling of animal and human tissues via UPLC-MS. *Nat Protocols*. 2013;8(1):17–32. doi:10.1038/nprot.2012.135
24. Wen B, Mei Z, Zeng C, Liu S. metaX: a flexible and comprehensive software for processing metabolomics data. *BMC Bioinf*. 2017;18(1):183. doi:10.1186/s12859-017-1579-y
25. Luo W, Brouwer C. Pathview: an R/Bioconductor package for pathway-based data integration and visualization. *Bioinformatics*. 2013;29 (14):1830–1831. doi:10.1093/bioinformatics/btt285
26. Csardi G, Nepusz T. The igraph software. *Complex Syst*. 2006;1695:1–9.
27. Luo W, Pant G, Bhavnasi YK, Blanchard SG, Brouwer C. Pathview web: user friendly pathway visualization and data integration. *Nucleic Acids Res*. 2017;45(W1):W501–W508. doi:10.1093/nar/gkx372
28. Judy RM, Sheedy CJ, Gardner BM. Insights into the structure and function of the Pex1/Pex6 AAA-ATPase in peroxisome homeostasis. *Cells*. 2022;11(13):2067. doi:10.3390/cells11132067
29. Bozkus F, San I, Ulas T, et al. Evaluation of total oxidative stress parameters in patients with nasal polyps. *Acta Otorhinolaryngologica Italica*. 2013;33(4):248–253.
30. Jin P, Zi X, Charn TC, et al. Histopathological features of antrochoanal polyps in Chinese patients. *Rhinology*. 2018;56(4):378–385. doi:10.4193/Rhin18.057
31. Islamoglu Y, Kesici GG, Canan Y, et al. Investigation of oxidative stress in antrochoanal polyp etiology. *Ear Nose Throat J*. 2020;99:633–636.
32. Wang H, Xu X, Lu H, et al. Identification of potential feature genes in CRSwNP using bioinformatics analysis and machine learning strategies. *J Inflamm Res*. 2024;17:7573–7590. doi:10.2147/JIR.S484914
33. Qiu H, Liu J, Wu Q, et al. An in vitro study of the impact of IL-17A and IL-22 on ciliogenesis in nasal polyps epithelium via the Hippo-YAP pathway. *J Allergy Clin Immunol*. 2024;154(5):1180–1194. doi:10.1016/j.jaci.2024.07.006
34. Dobzanski A, Khalil SM, Lane AP. Nasal polyp fibroblasts modulate epithelial characteristics via Wnt signaling. *Int Forum Allergy Rhinol*. 2018;8 (12):1412–1420. doi:10.1002/alr.22199
35. Mostafa HS, Fawzy TO, Jabri WR, Ayad E. Lymphatic obstruction: a novel etiologic factor in the formation of antrochoanal polyps. *Ann Otol Rhinol Laryngol*. 2014;123(6):381–386. doi:10.1177/0003489414522973
36. Shin K, Lee SH. Interplay between Inflammatory Responses and Lymphatic Vessels. *Immun Net*. 2014;14(4):182–186. doi:10.4110/in.2014.14.4.182